PHYSICS AND CHEMISTRY OF SOLID STATE
V. 24, No. 3 (2023) pp. 433-440
Section: Technology

DOI: 10.15330/pcss.24.3.433-440

Vasyl Stefanyk Precarpathian National University

ФІЗИКА І ХІМІЯ ТВЕРДОГО ТІЛА
Т. 24, № 3 (2023) С. 433-440
Технічні науки

PACS: 75.76.+j. ISSN 1729-4428

R.L. Politanskyi[1], P.M. Shpatar[1], M.V. Vistak[2], I.T. Kogut[3], I.S. Diskovskyi[2], Yu.A. Rudyak[4]

Electromagnetic Field Detectors Based on Spintronics Devices

[1]*Yuriy Fedkovych Chernivtsi National University, Chernivtsi, Ukraine, r.politansky@chnu.edu.ua, p.shpatar@chnu.edu.ua;*
[2]*Danylo Halytsky Lviv National Medical University, Lviv, Ukraine, vistak_maria@ukr.net, diskovkyi@gmal.com;*
[3]*Vasyl Stefanyk Precarpathian National University, Ivano-Frankivsk, Ukraine, igor.kohut@pnu.edu.ua;*
[4] *Ivan Horbachevsky Ternopil National Medical University, Ternopil, Ukraine, rydjakya@tdmu.edu.ua.*

The paper proposes a model of an electromagnetic radiation sensor that uses the precession of the magnetization vector in a ferromagnet (ferromagnetic resonance) as a result of absorbing the energy of an incident electromagnetic wave, the generation of a spin current as a result of this precession, the generation of a spin-polarized current as a result of the passage of a spin current in a non-magnetic metal, and a change in the direction of magnetization of a ferromagnetic layer with a low coercive force (free layer) due to the passage of a spin-polarized current. Then the radiation will be detected by its effect on the electrical resistance of the entire structure, which depends on the mutual directions (parallel or antiparallel) of magnetization of the free and fixed (with a large coercive force) ferromagnetic layers (phenomenon of giant magnetic resistance). The dependence of the spin-polarized current in the device on the frequency and amplitude of the incident electromagnetic wave with linear polarization was calculated. A method of calculating the range of amplitude and frequency values of radiation that can be detected by the sensor has been developed. The parameters of this model are the detection time and the number of spin gates in one sensor. Calculations are given for a ferromagnetic layer made of permalloy and for spin valves with four different critical current values that determine the process of remagnetization of the free layer: 20, 50, 100, and 200 microamps.

Keywords: electromagnetic field sensor, ferromagnetic resonance, spin current generation, spin valve.

Received 25 April 2023; Accepted 21 August 2023.

Introduction

Spintronics devices are widely used in those fields of science and technology where the task of detecting weak signals in complex electromagnetic conditions is important. This is due, first of all, to the ability to significantly reduce, or practically reduce to zero, disturbances caused by induced external and hardware-generated thermal noise. The rapid development and improvement of nanotechnology enables the practical implementation of fundamental research in the field of spintronics aimed at the design of electromagnetic radiation detection devices based on new physical laws and regularities. Conducting promising research makes it possible to create highly intelligent sensors of the electromagnetic field, which allow to simultaneously obtain temporal and spatial characteristics of this field with the formation of a digital signal already at the stage of detection.

One of the most promising applications of spintronics devices is the detection of weak signals of the electromagnetic field in the conditions of the superimposition of powerful noise-like interference signals. Numerous studies are being conducted in this direction with the aim of using highly sensitive electromagnetic field sensors in various fields of science and technology. They are used to detect electromagnetic field sources that have various causes: biological organisms, industrial objects, current sources and conductors in cars, power lines, etc. [1-3]. In addition, spintronics devices can be used to measure and detect thermal fields, including those caused by infrared radiation, thanks to the phenomenon of spin induction

under the influence of temperature gradients [4, 5]. Highly sensitive electromagnetic field sensors are particularly effective in medical applications, as are optical range detectors [6-12]. The phenomenon of ferromagnetic resonance can be used to detect signals with binary modulation [13], i.e. it is potentially suitable for use in receiving devices of high-frequency signals with a frequency of tens of gigahertz. Generating high-frequency oscillations is as important a scientific and technical task as their detection [14, 15]. The phenomenon of ferromagnetic resonance is also the basis for the generation of electromagnetic radiation by the method of spin oscillators, which is used in advanced information recording devices [16].

Provided there is a favourable relationship between the frequency and direction of the external electromagnetic wave, the applied constant magnetic field and the characteristics of the material from which the outer ferromagnetic layer of the sensor is made, a long-term non-damping precession of local magnetization (ferromagnetic resonance) occurs [17, 18]. As a result, there is a constant exchange between the angular magnetic moment of the local magnetization of the ferromagnet and the spin moments of the conduction electrons. This is how a spin current arises - a directed flow of the spin angular momentum of conduction electrons, which may not be accompanied by a directed movement of electrons (pure spin current).

Next after the ferromagnetic resonance, there is a functional unit for generating a spin-polarized current in a non-magnetic metal adjacent to the ferromagnetic layer. As a result, a potential difference occurs in the external permanent magnetic field. This phenomenon is known as the inverse spin Hall effect. By measuring this potential difference, electromagnetic radiation can be detected [19]. But at the same time, it becomes necessary to measure very small values of the voltage, which is tenths of a millivolt. This low voltage can be compared to thermal noise voltage fluctuations, unless ultra-low temperatures are used.

We proposed a new method, which is based on passing the spin-polarized current, generated as a result of the mechanisms described above, through a device called a spin valve [20]. The spin-polarized current causes a change in the state of the spin valve (giant magnetoresistance effect). Research makes it possible to determine the range of frequency and amplitude values of electromagnetic radiation that can be detected by the proposed device.

I. Scheme of the sensor design and spin current generation

In Fig. 1 shows the part of the device sensitive to electromagnetic detection in different projections (Fig. 1a shows the front view, and Fig. 1b shows its cross-section).

The ferromagnetic layer, in which precession occurs, is a square with a size of 1×0.4 мм^2 in cross section, the thickness of the layer is 10 nm [21]. The spin valve is a cylinder, the diameter of its cross section is about 50 nm [22]. Then the area of one valve is $S_0 = 1.963 \cdot 10^{-15}$м^2, and this value is used in further calculations. Based on the ratio of geometric dimensions, it can be understood that one sensor can contain up to one million spin valves. This greatly increases the probability of detection, but the complexity of connecting contacts to each individual valve limits this number. However, the reliability of the device remains high, even if the number of valves is hundreds of units. This is obviously due to the fact that all the valves are turned on in parallel, so the reliability of the sensor increases significantly.

Consider the processes that occur during the interaction of the sensor with external electromagnetic radiation. First, under the action of the variable magnetic field of the incident electromagnetic wave in the outer ferromagnetic layer (layer 2 in Fig. 1), the precession of the magnetic moment occurs. At the same time, a spin current arises, which can be transmitted to the adjacent layer of non-magnetic metal (layer 2 in Fig. 1). In a non-magnetic metal, a spin-polarized current is generated under the action of a spin current. In the next

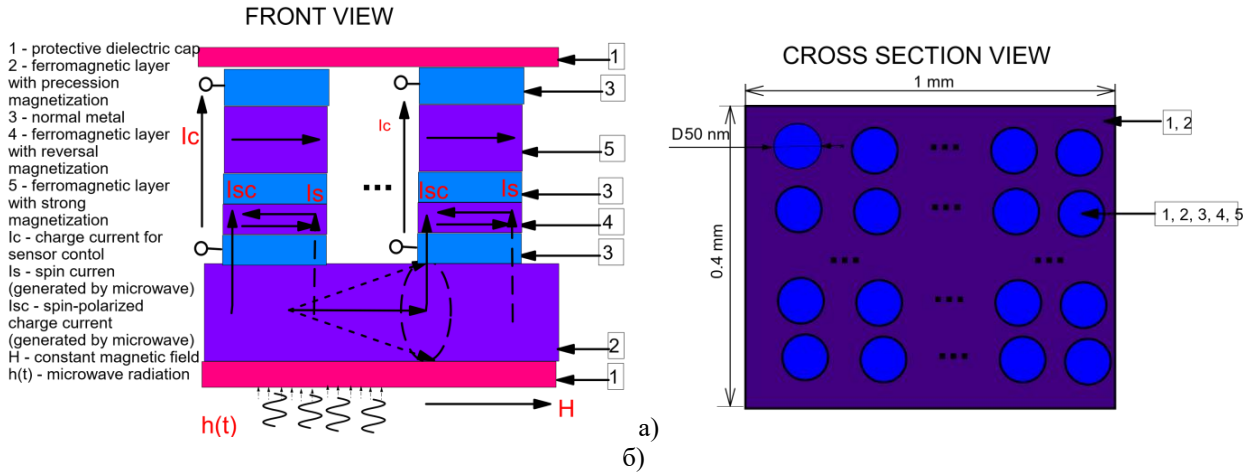

Fig. 1. Electromagnetic field spin sensor: a) – front view (1 – protective layer; 2 – magnetic layer with a weak coercive force, where precession of the magnetization vector occurs; 3 – non-magnetic metal; 4 – freely remagnetized magnetic layer (in the plane of the sample); 5 – magnetic layer with fixed magnetization in the plane of the sample); b) cross section and its geometric dimensions (1, 2 – protective layer and outer ferromagnetic layer, 3, 4 and 5 – nanoscale spin valve structures).

ferromagnetic layer (4 in Fig. 1), which has a low coercive force, the direction of magnetization changes under the action of a spin-polarized current. Then the ferromagnetic layers (4 and 5 in Fig. 1), which, together with the non-magnetic metal that separates them, form a spin valve, acquire opposite directions of magnetization in the plane of the sample. This leads to a significant increase in the electrical resistance of the entire structure [20]. In order to restore the sensor's ability to detect, it is necessary to change the direction of magnetization of the ferromagnetic layer again (4 in Fig. 1). This can be achieved by passing an electric current in the opposite direction. Then a spin current arises in the ferromagnetic layer 5, which flows into the adjacent layer of a non-magnetic metal, in which a spin-polarized current is generated. Under its action, the direction of magnetization in the ferromagnetic layer (4 in Fig. 1) becomes the same as the direction of magnetization of another ferromagnetic layer (5 in Fig. 1). Thus, the electrical resistance of the entire structure becomes low again.

As already mentioned above, the flow of spin angular momentum can be simulated by a spin current. To estimate its value, a model of a single-domain ferromagnetic layer that absorbs electromagnetic radiation in an external permanent magnetic field is used [21]. This model is based on the Landau-Lifshitz-Hilbert equation (1):

$$\frac{\partial \hat{M}}{\partial t} = -\gamma \hat{M} \times \vec{H}_{eff} + \alpha \cdot \hat{M} \times \frac{\partial \hat{M}}{\partial t} - \frac{\gamma j_s^{SH}}{M_s d_F} \hat{M} \times (\hat{M} \times \hat{\sigma}), \quad (1)$$

where γ – the gyromagnetic ratio; $\hat{M}$ – the unit vector co-directed with the magnetization vector of the ferromagnetic layer $\vec{M}$ (single domain model); $\hat{\sigma}$ – the unit vector is co-directed with the spin-momentum flux vector; d_F – the thickness of the ferromagnetic layer; $\vec{H}_{eff}$ – the resulting magnetic field; M_s – the limit value of magnetization of the ferromagnetic layer (saturation value); α – the Hilbert damping factor.

The resulting magnetic field $\vec{H}_{eff}$ is formed by the superimposition of the external constant magnetic field $\vec{H}$, the ferromagnetic sample's own field, and the variable magnetic field $\vec{h}_{ac}(t)$:

$$\vec{H}_{eff} = \vec{H} - 4\pi M_s \hat{x} + \vec{h}_{ac}(t) = \vec{H} - 4\pi M_s \hat{x} + \\ + (0, h_{ac} e^{i\omega t}, 0). \quad (2)$$

The parameters of this model are the frequency ω and the amplitude h_{ac} of electromagnetic radiation, the direction and amplitude of the external permanent magnetic field $\vec{H}$, and the saturation magnetization of the ferromagnet M_s (layer 2 in Fig. 1).

The value of the spin current calculated according to this model [21] is determined by formula (3):

$$j_s = \frac{g_r^{\uparrow\downarrow} \gamma^2 h_{ac}^2 \hbar \cdot \left(4\pi M_s \cdot \gamma \cdot \sin^2\theta_M + \sqrt{(4\pi M_s)^2 \cdot \gamma^2 \cdot \sin^4\theta_M + 4\omega^2}\right)}{8\pi\alpha^2 [(4\pi M_s)^2 \cdot \gamma^2 \cdot \sin^4\theta_M + 4\omega^2]} \quad (3)$$

where $g_r^{\uparrow\downarrow}$ – the spin conduction on the «ferromagnet-pure metal» surface; θ_M – the angle between the normal to the plane of the structure and the precession axis of the magnetization vector of the ferromagnetic layer (Fig. 2a). The dependence of the precession angle of the magnetization vector on the direction of the external magnetic field in the case of ferromagnetic resonance is shown in Fig. 2b [21].

II. Selection of the direction of the permanent magnetic field and calculation of the spin-polarized current

In accordance with the purpose of detecting external radiation, it is necessary to maximize the component of the spin current directed perpendicular to the plane of the layer (vertically upwards in Fig. 2a). This can be achieved by choosing the angle θ_H, which indicates the direction of the permanent magnetic field, while the value of the angle θ_M is found according to the functional dependence, the graph of which is shown in Fig. 2b.

The spin current is directed parallel to the plane in which the end of the magnetization vector rotates (coloured in red in Fig. 2a). Thus, the parameter of the detection system θ_H should be chosen so that the value of the vertical component of the spin current j_{SZ} is maximum (4):

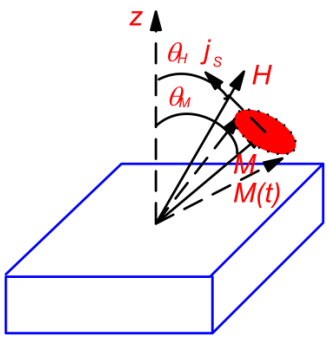

а)

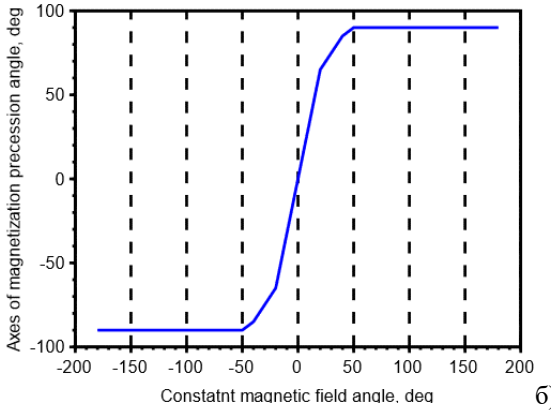

б)

Fig. 2. The direction θ_H of the external constant magnetic field $\vec{H}$, the precession angle θ_M of the magnetization vector $\vec{M}$ and the spin current $\vec{j}_S$ (a); the dependence of the angle θ_M on the angle θ_H (b).

$$j_{sz} = j_s \cdot cos(\theta_M) = \max_{-180° \le \theta_H \le 180°} \{j_s \cdot cos(f(\theta_H))\} \quad (4)$$

Based on the analysis of the optimization problem (4), it was concluded that the optimal value of the angles of the direction of the constant magnetic field and the precession of the magnetization vector is 90°: $\theta_{Hopt} = \theta_{Mopt} = 90°$ for the entire frequency and amplitude range under investigation. This means that for a constant magnetic field directed parallel to the plane of the ferromagnetic layer (horizontally in Fig. 2a), the precession vector is also directed horizontally, and the generated spin current is directed vertically. Then all the generated spin current passes into the non-magnetic metal layer (3 in Fig. 1), thus the value of the spin-polarized current is also maximum. Optimal solutions of problem (4) are also other angles exceeding 90° ($90° < \theta_{Hopt} < 180°$, $\theta_{Mopt} = 90°$). But, in our opinion, this significantly complicates the design of the sensor.

The values of numerical constants and characteristics of "ferromagnetic-nonmagnetic metal" materials for $Ni_{81}Fe_{19}$/Pt, which are given in [21], are used for the calculations:

- the spin conductivity: $g_r^{\uparrow\downarrow} = 2.31 \cdot 10^{19} m^{-2}$ (for the surface $Ni_{81}Fe_{19}$/Pt);
- the electron gyromagnetic ratio: $\gamma = 1.86 \cdot 10^{11}\, {}^{1}/_{T \cdot s}$ (for the $Ni_{81}Fe_{19}$);
- the magnetization of a ferromagnet in the saturation: $4\pi M_s = 0.754\ T$ (for $Ni_{81}Fe_{19}$);
- the Hilbert damping coefficient: $\alpha = 0.02$ (for $Ni_{81}Fe_{19}$);
- the Planck's constant: $\hbar = 1.054 \cdot 10^{-34} J \cdot s$;
- the charge of an electron: $e = 1.6 \cdot 10^{-19}\ C$.

For these parameters, the values of spin current caused by electromagnetic radiation in the frequency range from 1 to 50 gigahertz and amplitude from 5 to 50 millitesla are calculated. Such values of the frequency and amplitude of radiation are selected based on the analysis of many references, where the results of an experimental study of the phenomenon of ferromagnetic resonance are given. The vast majority of experimental data determine the frequency at which ferromagnetic resonance is observed at 1 - 15 GHz [23-25], there are also data that ferromagnetic resonance can be observed at frequencies of several tens of gigahertz [26], and for hard magnetic materials such as hexaferrites or iron-gallium alloys, the resonant frequency can reach as much as 35 GHz [27]. The highest subterahertz frequencies for which spin induction caused by the absorption of electromagnetic radiation is experimentally detected are published for antiferromagnetic materials (the so-called antiferromagnetic resonance) [28]. The largest calculated value of the spin current for the investigated ranges of frequencies and amplitudes is $1.67 \cdot 10^{-3} J/m^2$, and the least is $4 \cdot 10^{-7} J/m^2$.

Silicon-on-insulator (SI) structures appear to be promising components of electromagnetic field detectors based on spintronics devices in an integrated design as intelligent sensors or microsystems-on-a-crystal, which, according to the results of research, have extremely high coefficients of magnetic sensitivity in a wide range of temperatures, including cryogenic ones, and also have improved possibilities for designing 3D instrument structures [29, 30].

III. Determination of the operating range of frequencies and amplitudes

We use the method described in [31] to calculate the reliability of the sensor and the operating ranges of the frequency and amplitude of radiation. The probability of an error can be quantitatively characterized by the probability that the spin valve will not change its state (parallel or antiparallel directions of layers 4 and 5 in Fig. 1) under the action of the spin-polarized current I_c during the time interval τ. The error that occurs due to a spontaneous change in the state of the valve, without the application of external radiation, is not taken into account.

The value of the density of the spin-polarized current, which is formed in the non-magnetic metal (layer 3 in Fig. 1), and then passes through the spin valve, depends on the thickness and material of the non-magnetic metal layer [21]:

$$j_c = \theta_{SHE} \left(\frac{2e}{\hbar}\right) \frac{\lambda_N}{d_N} tanh\left(\frac{2d_N}{\lambda_N}\right) j_s, \quad (4)$$

where j_c – the current density that passes into ferromagnetic layer 4, which changes the direction of magnetization (layer 4 in Fig. 1), j_s – the spin current generated as a result of the precession in the outer ferromagnetic layer (2 in Fig. 1), and which is determined by (3), θ_{SHE} – the spin Hall angle, λ_N – the spin diffusion length in a nonmagnetic metal, d_N – its thickness.

Next, we use the following characteristics of a non-magnetic metal [21]:

- $\theta_{SHE} = 0.04$ (Pt);
- довжина спінової дифузії: $\lambda_N = 10$ нм (Pt);
- товщина: $d_N = 10$ нм(Pt).

Then the largest and smallest spin-polarized current densities are $1.951 \cdot 10^{11}$ А/м^2 and $4.242 \cdot 10^{7}$ А/м^2, respectively. After multiplying the obtained values by the area of one valve S_0, we find the current passing through each valve. Thus, the largest and smallest calculated current values are 383 microamps and 80 nanoamps, respectively. This significantly limits the permissible values of frequencies and amplitudes of detected radiation, since the value of the critical current at which remagnetization occurs is tens of microamperes for most ferromagnetic materials used in spin valves. An increase in the amplitude of the external radiation leads to an increase in the spin current, and therefore the current passing through each spin gate. Whereas an increase in frequency leads to its decrease. This regularity is illustrated by the graph shown in Fig. 3, which is built on the basis of the dependence of the current passing through one spin valve on the frequency and amplitude of radiation.

According to the model for calculating the reliability of device operation [31], the probability that remagnetization will not occur (false decision regarding the presence of radiation) is determined by the expression:

$$p_{err}(I_c, \tau) = 148 \cdot exp\left[-\frac{2\tau}{\tau_0} \cdot (I_c/I_{0c} - 1)\right], \quad (5)$$

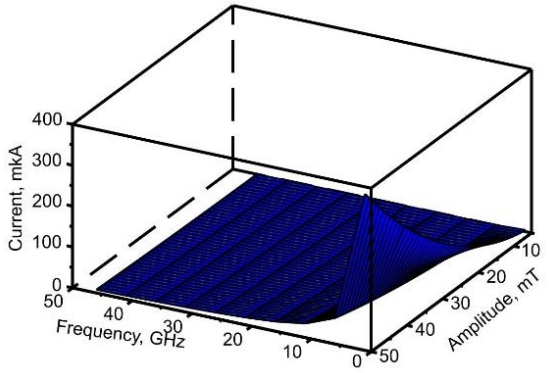

Fig. 3. Dependence of the current passing through one valve on the frequency and amplitude of microwave radiation.

This model has two parameters: critical current I_{0c} and time constant τ_0. The value of the critical current determines the smallest value of the spin-polarized current I_c, at which remagnetization can occur. The variable τ means the duration of the detection process. Another limitation of this model is the obvious condition that $p_{err}(I_c, \tau) \leq 1$. Therefore, there is also a limit on the smallest possible detection time, which depends on the ratio I_c/I_{0c}:

$$\tau_{min} \geq \frac{ln(p_{err}/148) \cdot \tau_0}{2 \cdot (I_c/I_{0c} - 1)} \quad .(6)$$

It is obvious that the range of permissible amplitude and frequency of radiation that can be detected by the sensor is limited by the value of the spin-polarized current passing through each valve, since it must exceed a critical value I_{0c}. For the critical value of the current density, different values are given, depending on the material of the remagnetized layer (4 in Fig. 1) and the current polarization coefficient: it ranges from ultra-low values o 10^{10} А/м^2 [32] to larger values $(1 \div 4) \cdot 10^{11}$ А/м^2 [33]. By multiplying the value of the critical current density by the area of one spin valve, we determine the value of the critical current. To further determine the ranges of amplitude and frequency of radiation, we use four values for the critical current: $I_{0c1} = 20\ \mu A$, $I_{0c2} = 50\ \mu A$, $I_{0c3} = 100\ \mu A$, $I_{0c4} = 200\ \mu A$. Graphs reflecting the results of these calculations are shown in Fig. 4.

The value of the time constant of the process in formula (5), calculated under the condition of room temperature is $\tau_0 = 8$ нс [31]. Thus, the calculated frequency and amplitude ranges correspond to the operation of the sensor at room temperature. The variables of the model to be optimized are the reliability of the device, determined by the probability $p = 1 - p_{err}$, and the detection time τ, which are selected for the given values of the frequency and amplitude of radiation. The value of the critical current is selected in accordance with the diagram shown in Fig. 4. Compared with previous studies [31], the formula for calculating reliability should be changed, since detection occurs immediately by all spin gates at the same time (Fig. 1a, 1b):

$$p = 1 - (p_{err})^n, \quad (7)$$

where n – the number of spin valves in one sensor.

The developed model makes it possible to estimate the most important for practical application characteristic of the detection process: the minimum necessary for a given frequency of an electromagnetic wave, the amplitude of its magnetic field. This is illustrated by the graph shown in Fig. 5. The amplitude of the external permanent magnetic field $\vec{H}$ is determined by the condition of the existence of ferromagnetic resonance in accordance with numerous experimental data.

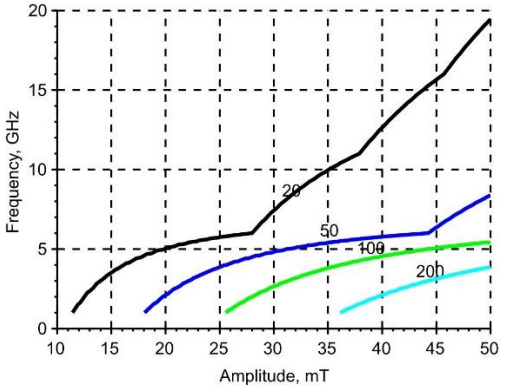

Fig. 4. Ranges of frequency and amplitude for critical current of 20, 50, 100 and 200 microamps.

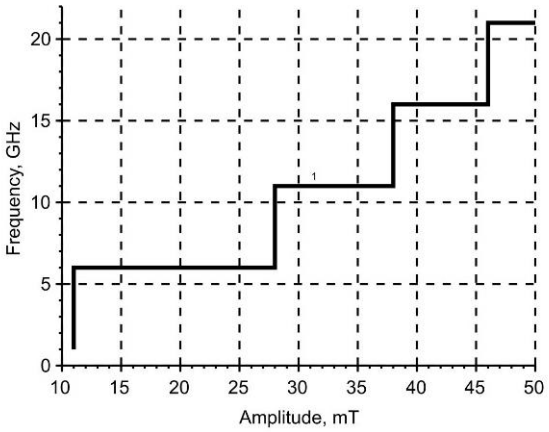

Fig. 5. Diagram of the dependence of the minimum amplitude required for detection on the radiation frequency.

Jump-like transitions in the diagram shown in Fig. 5, determined by the method of choosing the critical current, the value of which significantly affects the probability of an error calculated by relation (7). This value was chosen in accordance with the diagram shown in Fig. 4, that is, the minimum necessary value of the critical current is chosen from the four possible values I_{0c1}, I_{0c2}, I_{0c3}, I_{0c4} that were discussed above. For this method of selecting the critical current in models (5) and (7), the "amplitude-frequency" diagrams, calculated for different number of valves n and detection duration τ, practically do not differ.

IV. Discussion of results and conclusions

Highly sensitive sensors can significantly expand the scope of applications of IoT devices and other cyber-physical systems, where electromagnetic field emitters with different radii are used. After all, improving one of the most important characteristics of electromagnetic field detection devices – the signal/noise ratio can significantly reduce the power consumption of transmitters, and lead to their miniaturization and increase the speed of data transmission. The use of fundamentally new methods of digital signal processing will significantly expand the possibilities of application, protection against attacks and the possibility of functioning in the conditions of complex electromagnetic conditions of sensor networks of various levels of topological complexity and control technologies.

The paper describes the model of the electromagnetic field sensor device, which uses the phenomenon of spin current generation due to the precession of the magnetization vector of the ferromagnetic layer, which absorbs electromagnetic radiation. Based on the analysis of literary sources, it is concluded that it is possible to combine several phenomena related to the application of spin at once: generation of spin current, generation of spin-polarized current in a non-magnetic metal layer, remagnetization of a ferromagnetic layer with a small coercive force, reverse remagnetization due to passing a constant current in the reverse direction.

The researched method of detecting the external electromagnetic field has a number of advantages compared to traditional detection methods that use conventional antennas made of conductors: hardware losses due to thermal current and secondary radiation of the antenna are significantly reduced; potentially increases detection speed and accuracy, as the device makes it possible to generate a digital signal practically at the stage of electromagnetic field detection. The developed method of constructing the "amplitude-frequency" diagram allows designing information transmission systems that use high-frequency radiation to transmit information signals.

Politanskyi R.L. – Doctor of Technical Sciences, Professor, Professor of the Radio Engineering and Cyber Security Department;
Shpatar P.M. – Candidate of Technical Sciences, Associate Professor, Head of Radio Engineering and Cyber Security Department;
Vistak M.V. – Doctor of Technical Sciences, Professor, Professor of the Biophysics Department;
Kogut I.T. – Doctor of Technical Sciences, Professor, Head of the Computer Engineering and Electronics Department;
Diskovskyi I.S. **–** Candidate of Medical Sciences, Associate Professor Department of the Dermatology, Venereology;
Rudyak Yu. A. **–** Doctor of Technical Sciences, Professor, Head of the Department of Medical Physics of Diagnostic and Therapeutic Equipment.

.

[1] X. Liu, K.H. Lam, K. Zhu, C. Zheng, X. Li, Y. Du, C. Liu, P.W.T. Pong, *Overview of Spintronic Sensors with Internet of Things for Smart Living*, IEEE Transactions on Magnetics, 55(11), 0800222 (2019); https://doi.org/10.1109/TMAG.2019.2927457.
[2] Y. Chen, X. Wang, Z. Sun, H. Li, 2nd Asia Symposium on Quality Electronic Design (ASQED) (IEEE, Penang, Malaysia, 2010); https://doi.org/10.1109/ASQED.2010.5548244.
[3] A. Tanwear, X. Liang, Y. Liu, A. Vuckovic, R. Ghannam, T. Bohnert, E. Paz, P.P. Freitas, R. Ferreira, H. Heidari, *Spintronic Sensors Based on Magnetic Tunnel Junctions for Wireless Eye Movement Gesture Control*, IEEE Transactions on Biomedical Circuits and Systems, 14(6), 1299 (2020); https://doi.org/10.1109/TBCAS.2020.3027242.
[4] S.O. Kim, W.J. Kim, K.-J. Kim, S.-B. Choe, Y.M. Jang, S.H. Yoon, B.K. Cho, T.D. Lee, *Experimental Study of Thermally Activated Magnetization Reversal With a Spin-Transfer Torque in a Nanowire*," IEEE Trans. Magn., 44(11), 2531 (2008); https://doi.org/10.1109/TMAG.2008.2002419.
[5] S. Luo, N. Xu, Y. Wang, J. Hong, L. You, *Thermally Assisted Skyrmion Memory (TA-SKM)*, IEEE Electron Device Letters, 41(6), 932 (2020); https://doi.org/10.1109/LED.2020.2986312.
[6] R.L. Politanskyi, V.I. Gorbulik, I.T. Kogut, M.V. Vistak, *The Modeling of growth process on the surface of crystal*, Physics and Chemistry of Solid State, 23(2), 387 (2022); https://doi.org/10.15330/pcss.23.2.387-393.
[7] M.V. Vistak, V.E. Dmytrakh, Z.M. Mykytyuk, V.S. Petryshak, Y.Y. Horbenko, *A liquid crystal-based sensitive element for optical sensors of cholesterol*, Func. Mater., 24(4), 687 (2017); https://doi.org/10.15407/fm24.04.687.
[8] W. Wójcik, M. Vistak, Z. Mykytyuk, R. Politanskyi, I. Diskovskyi, O. Sushynskyi, I. Kremer, T. Prystay, A. Jaxylykova, I. Shedereyeva, *Technical solutions and SPICE modelling of optical sensors*, Przeglad Elektrotechniczny, 96(10), 102 (2020); https://doi.org/10.15199/48.2020.10.18.
[9] G.I. Barylo, R.L. Holyaka, I.I. Helzhynskyy, Z.Yu. Hotra, M.S. Ivakh, R.L. Politanskyi, *Modeling of organic light emitting structures*, Physics and Chemistry of Solid State, 21(3), 519 (2020); https://doi.org/10.15330/pcss.21.3.519-524.
[10] R.L. Politanskyi, M.V. Vistak, G.I. Barylo, A.S. Andrushchak, *Simulation of anti-reflecting dielectric films by the interference matrix method*, Opt. Mater., 102, 109782 (2020); https://doi.org/10.1016/j.optmat.2020.109782.
[11] Z. Hotra, A. Mahlovanyy, Z. Mykytyuk, H. Barylo, M. Vistak, I. Kremer, M. Ivakh, R. Politanskyi, IEEE XVth International Conference on the Perspective Technologies and Methods in MEMS Design (MEMSTECH) (IEEE, Polyana, Ukraine, 2019); https://doi.org/10.1109/MEMSTECH.2019.8817378.

[12] O. Sushynskyi, M. Vistak, V. Dmytrah, IEEE XIIVth International Conference on Modern Problems of Radio Engineering, Telecommunications and Computer Science (TCSET) (IEEE, Lviv, Ukraine, 2016); https://doi.org/10.1109/TCSET.2016.7452075.

[13] F. Duan, D. Abbott, *Binary modulated signal detection in a bistable receiver with stochastic resonance*, Physica A, 376, 173 (2007); https://doi.org/10.1016/j.physa.2006.10.046.

[14] R.L. Politansky, Z.M. Nytrebych, R.I. Petryshyn, I.T. Kogut, O.M. Malanchuk, M.V. Vistak, *Simulation of the Propagation of Electromagnetic Oscillations by the Method of the Modified Equation of the Telegraph Line*, Physics and Chemistry of Solid State, 22(1), 168 (2021); https://doi.org/10.15330/pcss.22.1.168-174.

[15] Z. Nytrebych, R. Politanskyi, O. Malanchuk, R. Petryshyn, M. Vistak, IEEE 16th International Conference on the Experience of Designing and Application of CAD Systems (CADSM) (Lviv, Ukraine, 2021); https://doi.org/10.1109/CADSM52681.2021.9385248.

[16] Y. Nakagawa, M. Takagishi, N. Narita, T. Nagasawa, G. Koizumi, W. Chen, S. Kawasaki, T. Roppongi, A. Takeo, T. Maeda, *Spin-torque oscillator with coupled out-of-plane oscillation layers for microwave-assisted magnetic recording: experimental, analytical, and numerical studies*, Appl. Phys. Lett., 122, 042403 (2023); https://doi.org/10.1063/5.0133921.

[17] Y. Tserkovnyak, A. Brataas, G.E.W. Bauer, *Enhanced Gilbert Damping in Thin Ferromagnetic Films*, Phys. Rev. Lett., 88, 117601 (2002); https://doi.org/10.1103/PhysRevLett.88.117601.

[18] A. Brataas, Y. Tserkovnyak, G.E.W. Bauer, B.I. Halperin, *Spin battery operated by ferromagnetic resonance*, Phys. Rev. B, 66, 060404R (2002); https://doi.org/10.1103/PhysRevB.66.060404.

[19] E. Saitoha, M. Ueda, H. Miyajima, *Conversion of spin current into charge current at room temperature*: *Inverse spin-Hall effect*, Appl. Phys. Lett., 88, 182509 (2006); https://doi.org/10.1063/1.2199473.

[20] R.L. Politanskyi, L.F. Politanskyi, I.I. Grygorchak, A.D. Veriga, *Modeling of Spin Valves of Magnetoresistive Fast-Acting Memory*, Journal of Nano- and Electronic Physics, 10(6), 06027 (2018); https://doi.org/10.21272/jnep.10(6).06027.

[21] Y. Xu, D.D. Awschalom, J. Nitta, Handbook of Spintornics (Springer, Dordrecht Heidelberg New York London, 2016).

[22] P. Kumar, A. Naeemi, *Benchmarking of spin-orbit torque vs spin-transfer torque devices*, Appl. Phys. Lett., 121, 112406 (2022); https://doi.org/10.1063/5.0101265.

[23] V. Vlaminck, J.E. Pearson, S.D. Bader, A. Hoffman, *Dependence of spin-pumping spin Hall effect measurement on layer thickness and stacking order*, Phys. Rev. B, 88, 064414 (2013); https://doi.org/10.1103/PhysRevB.88.064414.

[24] HuJun Jiao, Gerrit E. W. Bauer, *Spin Backflow and ac Voltage Generation by Spin Pumping and the Inverse Spin Hall Effect*, Phys. Rev. Lett., 110, 217602 (2013); https://doi.org/10.1103/PhysRevLett.110.217602.

[25] K. Karube, L. Peng, J. Massel, M. Hemmida, H.-A. K. von Nidda, I. Kézsmárki, Xiuzhen Yu, Y. Tokura, Y. Taguchi, *Doping Control of Magnetic Anisotropy for Stable Antiskyrmion Formation in Scheibersite $(Fe,Ni)_3P$ with S_4 symmetry*, Adv. Mater., 34(11), 2108770 (2022); https://doi.org/10.1002/adma.202108770.

[26] D.M. Burn, S. Zhang, K. Zhai, Y. Chai, Y. Sun, G. van der Laan, Th. Hesjedal, *Mode-Resolved Detection of Magnetization Dynamics Using X-ray Diffractive Ferromagnetic Resonance*, Nano Lett., 20(1), 345 (2020); https://doi.org/10.1021/acs.nanolett.9b03989.

[27] P. Bajracharya, V. Sharma, A. Johnson, R. C. Budhani, *Resonant precession of magnetization and precession-indused DC voltages in FeGaB thin films*, J. Phys. D Appl Phys, 55, 075303 (2022); https://doi.org/10.1088/1361-6463/ac34ab.

[28] M. Guo, R. Cheng, *Field-assisted sub-terahertz spin pumping and auto-oscillation in NiO*, Appl. Phys. Lett., 121, 02401 (2022); https://doi.org/10.1063/5.0097211.

[29] I.T. Kogut, A.A. Druzhinin, V.I. Holota, *3D SOI elements for system-on-chip applications*, Adv. Mat. Res., 276, 137 (2011); https://doi.org/10.4028/www.scientific.net/AMR.276.137.

[30] A. Druzhinin, I. Ostrovskii, Y. Khoverko, I. Kogut, V. Golota, *Nanoscale polysilicon in sensors of physical values at cryogenic temperatures*, J. Mater. Sci: Mater. in Electron., 29(10), 8364 (2018); https://doi.org/10.1007/s10854-018-8847-0.

[31] R. Politanskyi, M. Vistak, A. Veryga, T. Ruda, *Modelling of Spintronic Devices for Application in Random Access Memory*, Informatyka Automatyka Pomiary w Gospodarce i Ochronie Środowiska, 10(1), 62 (2020); https://doi.org/10.35784/iapgos.915.

[32] J.D. Costa, S. Guisan, B. Lacoste, A.S. Jenkins, T. Böhnert, M. Tarequzzaman, J. Borme, F.L. Deepak, E. Paz, J. Ventura, R. Ferreira, P.P. Freitas, *High power and low critical current density spin transfer torque nano-oscillators using MgO barriers with intermediate* thickness, Sci. Rep., 7, 7237 (2017); https://doi.org/10.1038/s41598-017-07762-z.

[33] D.H. Kang, M. Shin, *Critical switching current density* of *magnetic tunnel junction with shape perpendicular magnetic anisotropy through the combination of spin-transfer and spin-orbit torques*, Sci. Rep., 11, 22842 (2021); https://doi.org/10.1038/s41598-021-02185-3.

Р.Л. Політанський[1], П.М. Шпатар[1], М.В. Вісьтак[2], І.Т. Когут[3], І.С. Дісковський[2], Ю.А. Рудяк[4]

Детектори електромагнітного поля на основі пристроїв спінтроніки

[1]*Чернівецький національний університет імені Юрія Федьковича, м. Чернівці, Україна, r.politansky@chnu.edu.ua, p.shpatar@chnu.edu.ua;*
[2]*Львівський національний медичний університет імені Данила Галицького, м. Львів, Україна, vistak_maria@ukr.net, diskovkyi@gmal.com;*
[3]*Прикарпатський національний університет імені Василя Стефаника, м. Івано-Франківськ, Україна, igor.kohut@pnu.edu.ua;*
[4]*Тернопільський національний медичний університет імен І. Я. Горбачевського, м. Тернопіль, Україна, rydjakya@tdmu.edu.ua*

У роботі запропонована модель сенсора електромагнітного випромінювання, який використовує прецесію вектора намагніченості у феромагнетику (феромагнітний резонанс) внаслідок поглинання енергії падаючої електромагнітної хвилі, генерування спінового струму внаслідок цієї прецесії, генерування спін-поляризованого струму внаслідок проходження спінового струму у немагнітному металі, і зміну напряму намагніченості феромагнітного шару із низькою коерцитивною силою (вільного шару) внаслідок проходження спін-поляризованого струму. Тоді випромінювання детектуватиметься за його дією на електричний опір усієї структури, який залежить від взаємних напрямів (паралельні або антипаралельні) намагніченості вільного і закріпленого (із великою коерцитивною силою) феромагнітних шарів (явище гігантського магнітного опору). Розраховані залежності спін-поляризованого струму у пристрої від частоти та амплітуди падаючої електромагнітної хвилі із лінійною поляризацією. Розроблена методика розрахунку діапазону значень амплітуди і частоти випромінювання, яке може детектувати сенсор. Параметрами цієї моделі є час детектування і кількість спінових вентилів у одному сенсорі. Приведені розрахунки для феромагнітного шару, виготовленому із пермалою, та для спінових вентилів із чотирма різними значеннями критичного струму, які визначають процес перемагнічування вільного шару: 20, 50, 100 і 200 мікроампер.

Ключові слова: сенсор електромагнітного поля, феромагнітний резонанс, генерування спінового струму, спіновий вентиль.